

FRESH Bioprinting of Biodegradable Chitosan Thermosensitive Hydrogels

Maedeh Rahimnejad^{1, a}, Atma Adoungotchodo^{2, a}, Nicole Demarquette², Sophie Lerouge^{1, 2, a*}

¹Biomedical Engineering Institute, School of Medicine, Université de Montréal, Canada

²Department of Mechanical Engineering, École de technologie supérieure (ÉTS), Canada

^aResearch Centre, Centre Hospitalier de l'Université de Montréal (CRCHUM), Canada

*Corresponding author

E-mail: sophie.lerouge@etsmtl.ca

Abstract

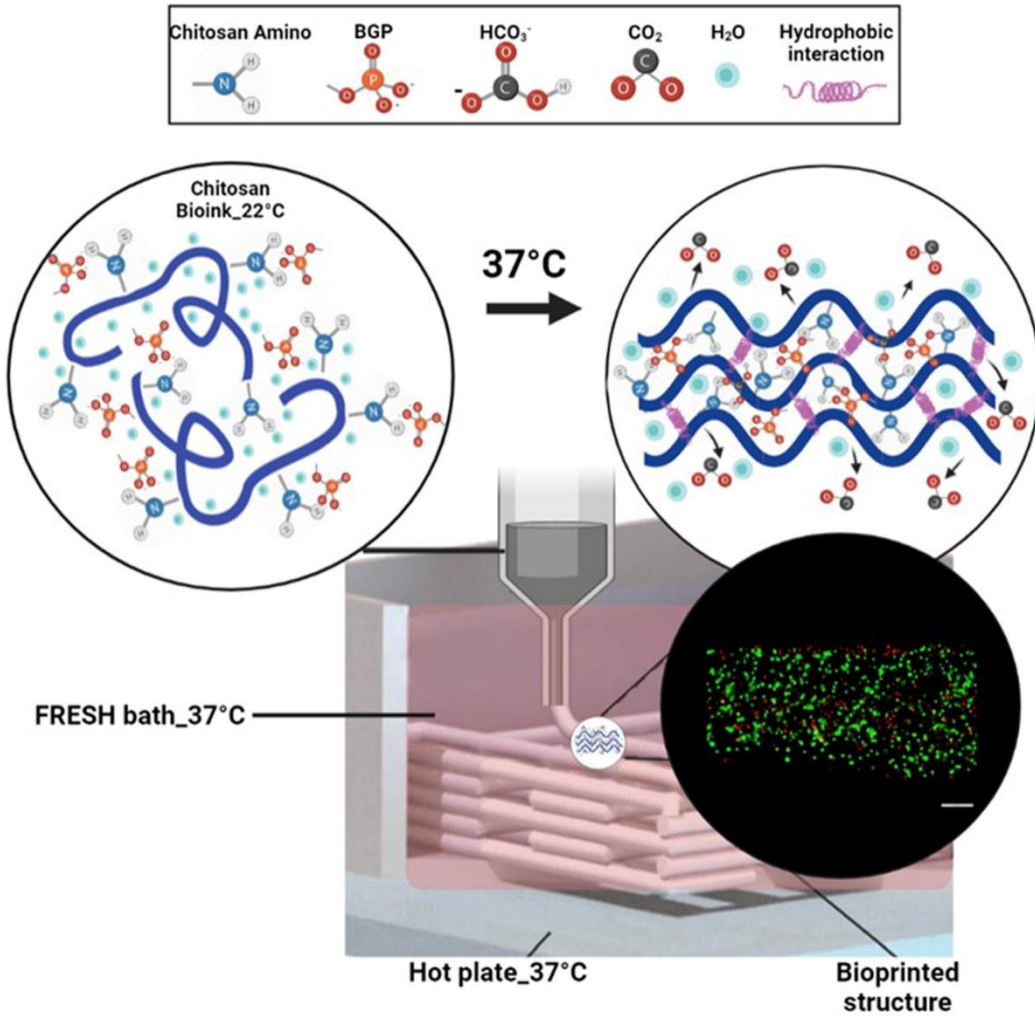
Thermosensitive chitosan (CH)-based hydrogels that rapidly pass from a liquid at room temperature to a mechanically stable solid at body temperature without any crosslinker show excellent potential for tissue engineering applications and could be interesting candidates for bioprinting. Unfortunately, since gelation is not instantaneous, formulations compatible with cell encapsulation (chitosan concentrations around 2% or lower) lead to very poor resolution and fidelity due to filament spreading.

Here, we investigate the FRESH bioprinting approach with a warm sacrificial support bath, to overcome these limitations and enhance the bioprintability of CH thermosensitive bioinks. First, a support bath, made of Pluronic including sodium chloride salt as a rheology modifier agent, was designed to meet the specific physical state requirements (solid at 37°C and liquid at room temperature) and rheological properties appropriate for bioprinting. This support bath presented yield stress of over 100 Pa, a shear thinning behavior, and fast self-healing during the cyclic recovery test. Three different chitosan hydrogels (CH2%, CH3%, and a mixture of CH and gelatin) were tested for their ability to form filament and 3D structures, with and without a support bath. Both the resolution and mechanical properties of the printed structure were drastically enhanced using the FRESH method, with an approximate fivefold decrease of the filament diameter which is close to the needle diameter. The printed structures were easily harvested without disturbing their shape by cooling the support bath. Live/dead assays confirmed that the viability of encapsulated mesenchymal stem cells was highest in CH2% and that the support bath-assisted bioprinting process did not adversely impact cell viability.

This study demonstrates that these thermosensitive chitosan-based bioinks could be good candidates for 3D bioprinting using advanced bioprinting approaches such as the FRESH method for various tissue engineering applications.

Keywords: bioink, thermosensitive chitosan-based hydrogel, support bath, FRESH bioprinting

Graphical abstract



Abbreviations:

BGP: Beta-glycerophosphate

CH: Chitosan

CH-Gel: chitosan-gelatin

FRESH: freeform reversible embedding of suspended hydrogels

G' : storage modulus

G'' : loss modulus

MSCs: Human bone marrow mesenchymal stems cells

SHC: Sodium-hydrogen-carbonate

1. Introduction

Despite the huge recent progress in bioprinting, the quest for better biodegradable bioinks is still ongoing. Chitosan thermosensitive physical hydrogels, that are liquid at room temperature, but rapidly gel at body temperature, present interesting features as bioinks [1-3]. In particular, it has been shown that when an acidic chitosan solution is mixed with a combination of Beta-glycerophosphate (BGP) and Sodium-hydrogen-carbonate (SHC), it forms a solution of physiological pH and osmolarity where cells and bioactive factors can easily be mixed. Once at 37°C, it rapidly gels into a strong macroporous hydrogel without the use of a chemical crosslinker [3]. Excellent survival of cells, such as mesenchymal stem cells, intervertebral disk cells, or T lymphocytes, to name just a few examples, was demonstrated and thanks to their good mechanical properties, these hydrogels have been already proposed for several cell therapy and tissue-engineering applications [4, 5].

Such thermosensitive hydrogels could overcome the limitations of cytotoxicity resulting from toxic crosslinkers or harsh non-physiological conditions. Moreover, chitosan is well known for its biocompatibility and is fully biodegradable, a significant advantage over alginate.

However, until now, it has not been possible to print 3D structures combining good fidelity and excellent cell viability with chitosan hydrogels. Previous work showed that (3%w/v) were necessary to result in structures with good resolution and handability [6]. This however led to a high mortality rate of encapsulated cells due to the high viscosity of the solution in which the cells were mixed and to the low porosity of the final hydrogel. Decreasing the chitosan to concentrations more suitable for cells (2% or below) resulted in poor shape-fidelity structures due to the low mechanical properties of the printed filaments (spreading under the weight of the overlying layers) [6-8]. The main reason for this is that the gelation process of chitosan hydrogel is not instantaneous. Moreover, to take advantage of the thermosensitivity of these hydrogels, it is important to maintain the environment at 37 °C. But keeping a simple warm substrate at 37 °C is quite challenging and can lead to water evaporation from the sample.

In this paper, we show how these limitations can be solved by taking advantage of the freeform reversible embedding of suspended hydrogels (FRESH) approach with a warm support bath. The FRESH method was initially proposed by Feinberg's team in 2015 [9] to maintain the intended structure during the print process and improve print fidelity. It is now largely used in the bioprinting field, with some amazing results, such as printing a full-size model of the heart [10, 11]. This method has been applied with several biopolymers such as alginate, collagen, and fibrin, but to the best of our knowledge, it has never been applied with chitosan.

The first objective of this work was to design a support bath that presents the key features required to print chitosan hydrogels. For that the support bath should present adequate rheological properties when warmed around 37 °C, to take advantage of the thermosensitivity of these hydrogels. It must be cytocompatible, and its removal after bioprinting should not impart any mechanical or biological shock to the cells. In terms of rheological properties, three main properties are desirable. First, the support bath should behave as a rigid body when subjected to

low stresses but flow as a viscous fluid when subjected to high stresses [12]. The rheological properties of such materials are generally described by the Herschel–Bulkley model [13, 14], where the shear stress τ relates to the shear rate $\dot{\gamma}$ as follows [15]:

$$\tau = \tau_0 + K\dot{\gamma}^n \quad (\text{Eq.1})$$

where τ_0 is the yield stress, below which the material behaves as a solid, K is the consistency index, and n , the flow behavior index. For $n < 1$ the material is shear-thinning, whereas for $n > 1$ it is shear-thickening. If $n = 1$, the model reduces to Bingham plastic fluid. It has been reported in the literature that the yield stress of the FRESH support should be equal to or higher than 100 Pa [14, 16].

Second, once the bioink is in place, the FRESH support should stop flowing and recover. Indeed, it should allow the bioink to place itself preventing to flow further. Furthermore, the recovery should be rapid to ensure no crevasses or air pockets are trailing from the moving nozzle [16]. Third, it has also been shown that the stiffness of the support bath, which can be accessed by its storage modulus G' , is of paramount importance to the process. Storage moduli of FRESH support should vary between 5,000 Pa to 10,000 Pa, to provide adequate support for a low viscosity ink and yet allow its penetration [11, 14, 17, 18].

Different materials have been proposed as a FRESH support bath, such as gelatin microparticles, Carbopol microgels and nanoclays (e.g., Laponite), and Pluronic. Gelatin microparticles (slurry) is the most commonly used material [9]. However, gelatin slurry is liquid at body temperature [10], which it is not suitable for chitosan bioinks that gel at 37 °C. Carbopol microgels are anionic [19] and not recommended for use with cationic hydrogels such as chitosan [20]. Nanoclays also are not suitable for cationic hydrogels, because possible positive charges dissolve the bath, and amine groups of chitosan can lead to the formation of small, flocculated particles, often described as “seeds” [21-23]. Another possible material for the FRESH method is Pluronic (F-127), a block copolymer, PEO-PPO-PEO, used alone or with additives [18, 24-27]. Pluronic is generally in the gel form at 37 °C, while liquid at lower temperatures, thus enabling its gentle removal by decreasing the temperature. Moreover, its gelation temperature and modulus can be tuned by varying its concentration and by the addition of salts, such as NaCl or CaCl₂ [14, 24, 28]. Thus, Pluronic is a promising FRESH support bath for this chitosan thermosensitive hydrogel.

This work aimed to study and optimize FRESH bioprinting of chitosan thermosensitive hydrogels using Pluronic as a support bath and to demonstrate how we can very significantly increase the printability of chitosan and chitosan-gelatin hydrogels and fabricate nice 3D structure with good mechanical properties and cytocompatibility.

2. Materials and Methods

2.1. Materials

Shrimp shell chitosan (ChitoClear, HQG110, Mw: 155 kDa, DDA 83%) was purchased from Primex (Iceland). β -Glycerol phosphate disodium salt pentahydrate (C₃H₇Na₂O₆P·5H₂O, hereafter BGP) was purchased from Sigma-Aldrich (Oakville, ON, Canada). Sodium hydrogen carbonate NaHCO₃ (sodium bicarbonate, hereafter SHC) was obtained from MP Biomedicals (Solon, OH, USA). Type A gelatin from porcine skin (G1890), Pluronic F-127

($M_w=12,600$ g/mol), and sodium chloride (NaCl) were purchased from Sigma-Aldrich. Other chemicals were of reagent grade and were used without further purification.

2.2. Chitosan and chitosan-gelatin bioinks preparation

Chitosan (CH) and chitosan-gelatin (CH-Gel) hydrogels were prepared by mixing an acidic CH or CH-Gel solution with a gelling agent solution at a volume ratio of 3:2, respectively. Chitosan (CH) powder was first solubilized in hydrochloric acid (HCl) (0.1 M) at 3.33% w/v (final concentration 2%), by way of mechanical stirring for 3 hours. For the chitosan-gelatin (CH-Gel) solution (final concentration 2% w/v for each component), gelatin powder was added to 0.1M HCl solution, heated to 37 °C for 30 min, then chitosan powder was added, and the solution was stirred for 4 hours. Chitosan solution at 5% w/v chitosan (in 0.015 M HCl; final CH 3% hydrogel) was also prepared as a control substance. The solutions were sterilized by autoclaving (20 min, 121 °C) and stored at 4 °C.

The gelling agent used in this study was a mixture of BGP and SHC, hereafter called BGP/SHC, at a final concentration in the hydrogel of 0.1 M/0.075 M and 0.15 M/0.113 M for 2% and 3% chitosan-based hydrogels, respectively, as previously published [2].

The two solutions were introduced in separate syringes, joined by a Luer lock connector. The content of the gelling agent syringe was pushed into the CH syringe, and the mixture was transferred back and forth from one syringe to another 15 times. Hydrogel solutions were then centrifuged to remove air bubbles and used immediately. Hydrogels had a final chitosan concentration of 2% (w/v) or 3% (w/v). All had a physiological pH.

2.3. FRESH bath preparation

Pluronic powder was solubilized under stirring in distilled water at concentrations of 17 to 23% w/v with and without 1% and 5% w/v NaCl salt for 6 hours at 4 °C. The pH and osmolality of the various solutions were measured using a Horiba LAQUAtwin pH-22 Compact and Portable pH Meter (Horiba, country), and Advanced® Micro 3300 Osmometer respectively.

2.4. Rheological characterization

Rheological characterization of the support bath and the bioinks were carried out using an Anton Paar instrument (Physica MCR 301, Germany) with a concentric cylinders type geometry (CC10/T200), 1 mm gap, or a cone-plate geometry (CP25) 25 mm in diameter. The linear viscoelastic (LVE) range was first determined using a plate-plate geometry (PP25) and an amplitude sweep test. The following tests were then performed, either on the support bath, the bioinks, or both:

- 1) Temperature sweep from 10°C to 45°C at a rate of 1 °C/min was first performed on various compositions of support bath, using the oscillatory mode in the LVE range, at a constant shear strain (1%) and constant frequency (1 Hz) to determine the formulations with adequate gelation temperature (temperature where the storage modulus G' was equal to the loss modulus G'').

- 2) Time sweeps at 37 °C were then performed to assess the stability and viscoelastic properties of the support bath. In addition, the gelation kinetics of the chitosan bioinks was studied using time sweep tests for 10 min at 22 °C (to assess their stability at room temperature in the printing cartridge) followed by 10 min at 37 °C (to assess their gelation kinetics once printed in the support bath).
- 3) Amplitude sweeps with strain-controlled mode (1% to 100% strain) were performed using oscillatory rheometry at a constant frequency (1Hz) to evaluate the yield stress of the hydrogels and support bath at 22 °C and 37 °C, respectively. The yield stress was considered as the stress value where G' dropped by >10% of the deformation.
- 4) Recovery tests at 37 °C were also performed using oscillatory rheometry, to verify the self-healing properties of the support bath after printing. The storage modulus of the bath was measured during various cycles mimicking the printing process: (1) Pre-printing (rest) (2 min at 1% strain); (2) Printing (sudden increase to 100% strain for 1 min) (3) Post printing (back to 1% strain). The hydrogels' recovery behavior was also evaluated with a slightly different protocol to factor in temperature after printing and take advantage of the hydrogel's thermosensitivity: (1) Pre-printing (1% strain for 10 min at 22°C); (2) Printing (100% strain for 1 min at 22°C); (3) Post-printing (1% strain for 10 min at 37°C).

2.5. Printing procedure

A 3D-Discovery bioprinter (RegenHU, Villaz-St-Pierre, Switzerland) was used to print the hydrogels via a plunger dispenser, which is able to maintain a constant dispensing rate (volume/min) during printing even if the hydrogel properties change with time. The cartridge was kept at room temperature, while the heated substrate (warm glass or warm FRESH bath) temperature was kept constant at 37 °C. A long stainless steel 25G needle (length: 25.4 mm; internal diameter = 0.26 mm) was used to print the hydrogels. The effect of the feed rate (3, 5, 7, 9, 11 mm/s) and flow rate (0.5, 1.0, 1.5 mm³/s) on filament width and continuity were first studied on glass (Figure S1 in supplemental data); then the optimal flow rate (0.5 mm³/s) was used to print within the bath.

2.6. Resolution and shape fidelity

Images of printed filaments were analyzed using the freeware ImageJ (Fiji.sc), according to the approach proposed by Gillispie et al. The average width [29] and the spreading ratio (printed filament width/ needle inner diameter) [30] were determined.

The best printing parameters (flow rate 0.5 mm³/s and feed rate 9 mm/s) were then used to print hydrogels on glass and within the FRESH bath in 10-layer and 20-layer gridded structures. The FRESH bath was removed 30 min after printing by putting samples at 4 °C for 10 min. Then, the printed structures were incubated once more for 24 hours at 37 °C. Their structural resolution and fidelity were assessed visually and quantified by two parameters: 1) the height of the printed structure was compared with its theoretical value (based on the layer-to-layer distance

corresponding to 80% of the needle's internal diameter); 2) the printability (Pr) based on square shape as proposed by Ouyang et al. [30] using the following equation:

$$Pr = \frac{L^2}{16A} \quad (\text{Eq.2})$$

where, L is the perimeter and A is the area of the printed squares in the gridded structure. For the ideal bioink, the Pr is close to 1, indicative of sharp angles and absence of filament spreading. The range of $0.9 < Pr < 1.1$ is considered as good printability [31].

2.7. Mechanical properties characterization

Unconfined compression tests were performed on 20-layer printed gridded structures using the MACH-1 testing device (Biomomentum, Canada). A velocity equal to 100% of the sample's height/min was used. The compressive strength and secant Young's modulus at 10% and 30% of deformation were calculated from the stress-strain curves. ImageJ software was used to calculate the actual surface area of the printed structure (without the holes in the structure) to determine the applied stress. Tests were performed at room temperature after 24 hours of sample incubation at 37 °C.

2.8. Bioprinting of stem cell loaded hydrogels

Human bone marrow mesenchymal stems cells (MSCs) (PT-2501, Lonza Inc., ON, Canada) were cultured in NutriStem XF (#cat 05-200-1A, Biological Industry, USA) supplemented with 0.6% NutriStem XF Supplement (#cat 05-201-1U, Biological Industry, USA). They were used at passage 6.

MSC were encapsulated in the hydrogels as follows: 1.2 mL of CH or CH-Gel solutions were first mixed with 0.4 mL gelling agent solution using two syringes (3 mL) connected with a Luer Lock. The obtained mixture was then mixed with 0.4 mL cell suspension (5×10^6 cells/mL). After mixing, the cell density was 10^6 cells/mL in a solution of 2% w/v chitosan with or without 2% w/v gelatin, 100 mM BGP and 75 mM SHC. A volume of 200 μ L of the solution was placed in a 48-well plate to be used as a control and to evaluate the effect of the printing process on cell viability. The solution remaining in the syringe was centrifuged at 1000 rpm for 1 min and used to bioprint different structures. Our bioprinter is stored in a biosafety cabinet and used in routine cell culture. All surfaces within the biosafety cabinet were disinfected with 70% ethanol and irradiated with the UV lamp overnight. Structures were bioprinted on the 6-well plate filled with a 1 ml 37 °C support bath. After bioprinting, the bath was removed for a 5 min incubation at 4 °C with a cold PBS buffer. Then, MEM α media (#cat 12561056, Gibco) supplemented with 10% FBS, and 1% penicillin/streptomycin was added to the surface and left to incubate 24 h at 37 °C, 5% CO₂. As a second control to evaluate the effect of the bath on cell viability, 200 μ l of the solution remaining in the cartridge after the bioprinting process was injected through the needle into an empty 48-well plate and treated similarly.

Cell viability was assessed after 24h. In short, the wells were washed twice with PBS and incubated for 45 min at 37 °C with serum-free medium supplemented with 2 μ M ethidium homodimer-3 and

1 μM calcein AM (LIVE/DEAD Cell imaging kit reagents, R37601, Life Technologies, Carlsbad, USA). The samples were then washed again with PBS and immediately observed using an inverted fluorescent microscope (Leica DM IRB, Feasterville, USA). Cell viability was calculated as the ratio of live cells (green) to total number of cells (green and red). The tally was obtained using the Analyze Particles function in ImageJ (National Institute of Health, USA).

2.9. Statistical analyses

All experiments were performed in triplicate. Results were expressed as mean \pm SD. Statistical analysis was performed using GraphPad Prism 7.04 software. One-way ANOVA and Tukey's multiple comparison tests were used to compare multiple groups. $P < 0.05$ was deemed statistically significant.

3. Results and Discussion

3.1. FRESH bath optimization and characterization

As explained in the introduction, the support bath was first designed to suit the specific needs of chitosan thermosensitive hydrogels, i.e. it must be a shear thinning at 37 °C (to provide support during the printing and rapid gelation of the chitosan hydrogel), heal well (recovery after strain), and then liquefy at a temperature that permits the easy removal of the cells.

Temperature sweeps and time sweep at 37°C confirmed that the gelation temperature and storage modulus (G') could be fine-tuned by changing the concentration of Pluronic [32-35] and NaCl [14, 24, 28, 36]. Main data are shown in Figure S2. Pluronic19%+1% NaCl was chosen as a support bath for further studies since it is completely liquid at 22 °C but forms a completely gelled and stable structure at temperatures above 32 °C with a storage modulus around 5 kPa (Figure 1). This allows for a safety margin in case the temperature of the support bath slightly decreases below 37°C, due to contact with ambient air. Moreover, NaCl 1% effectively provides osmolality to the support bath to a level similar to that of the printed material (physiological level) (323 ± 17 mOsm/kg H₂O (physiological level is deemed around 330 mOsm/kg)), in order to avoid osmotic exchange between the two. The support bath also had a physiological pH.

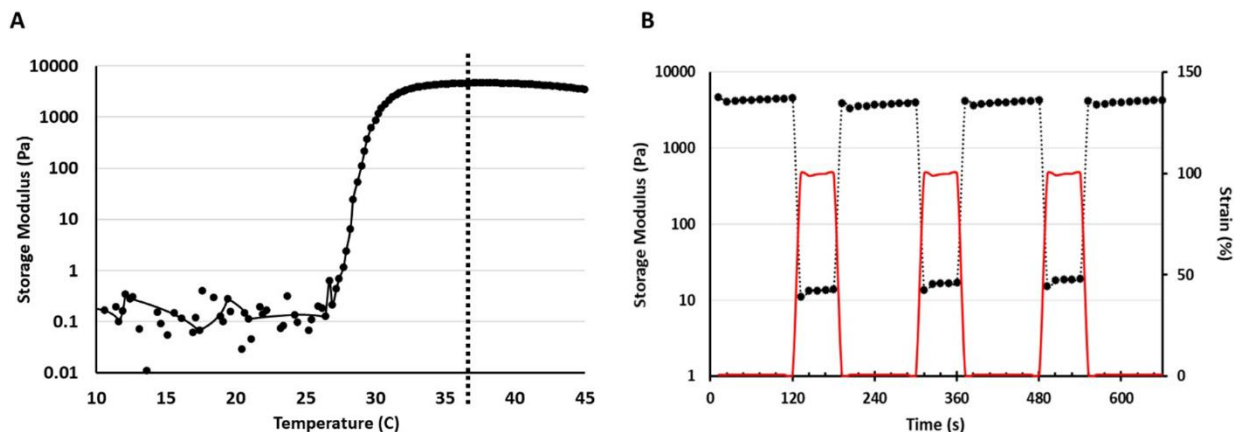


Figure 1. Rheological properties of Pluronic support bath A) Temperature ramps (10-45 °C) of Pluronic 19% (w/v) +1% (w/v) NaCl (dotted line=37°C); B) Recovery tests: Storage modulus of Pluronic 19% + 1% NaCl (black curve) during various cycles of strain at 37 °C (2 min rest at 1% strain, 1 min under shear at 100% strain, red curve) (mean; n≥3).

The support bath in the FRESH approach should also present sufficient yield stress to firmly hold the printed bioink after deposition while maintaining a shear-thinning behavior (so that it will not hinder the movement of the printing needle) and rapid recovery to a solid state after printing. Therefore, the support bath material's yield stress values, shear-thinning behavior, and self-healing were investigated. The optimized FRESH bath presents a yield stress of over 100 Pa (147 ± 3 Pa) (Figure S3). The Herschel-Bulkley model (Eq. 1) was used to fit the data and estimate the consistency index K and flow behavior index n ($n=0.15$; $K=147$; Figure S4). The recovery properties of the FRESH bath at 37°C was demonstrated throughout cyclic deformation (1 min under shear at 100% strain followed by 2 min rest) (Figure 1B). Even after various cycles, the material showed complete recovery (storage modulus coming immediately back to its previous value). Such rapid recovery to a solid state ensures that the extruded bioink is soundly embedded [14, 37].

3.2. Rheological behavior of chitosan-based hydrogel bioinks

Prior to bioprinting, the rheological properties of the chitosan-based bioinks were assessed to confirm their thermosensitivity, as well as their shear thinning and recovery behavior. Figure 2 shows the evolution of the storage modulus during time sweeps, first at room temperature (22 °C) for 10 min to estimate the stability of the hydrogel solutions in the printer cartridge, and then at a temperature varying to 37 °C to assess their gelation kinetics once on the heated glass or in the warm FRESH bath.

As previously published, CH2 shows a drastic increase of G' when the temperature increases to 37 °C, indicative of the gel's thermosensitivity. This suggests that a warm FRESH bath can help ensure rapid gelation during printing. When gelatin was added to chitosan (CH-Gel), the behavior was quite similar, except for the sudden drop of the storage modulus when the temperature was increased to 37 °C, probably due to the gelatin melting. In contrast, CH3 showed a different trend, with a continuous increase of G' value as a function of time, with only a minor influence due to the temperature rise to 37 °C.

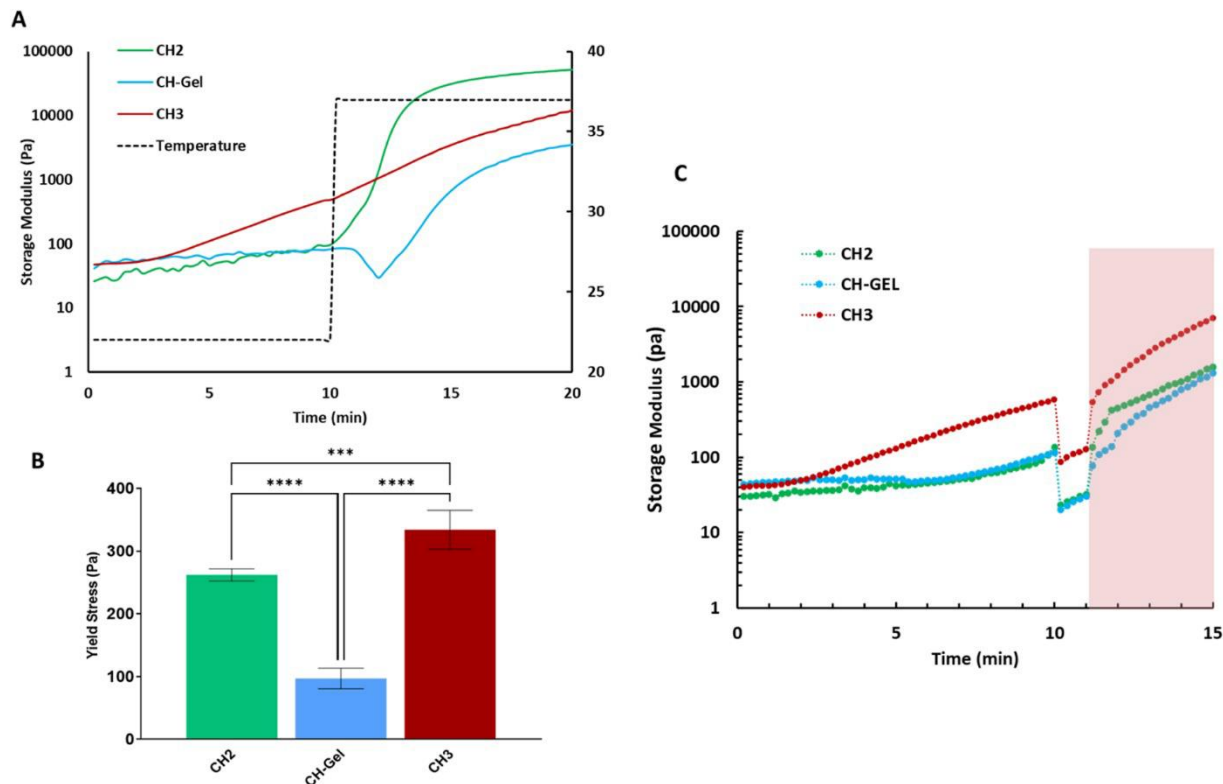


Figure 2. Rheological properties of chitosan hydrogels ; A) Evolution of the storage (G') and loss (G'') moduli of hydrogels as a function of time and following the sudden increase of the temperature from 22 to 37 °C (the dotted black line represents the temperature as a function of time).; CH2: chitosan 2% w/v hydrogel; CH3 : chitosan 3% w/v hydrogel; CH-Gel: chitosan 2% w/v gelatin hydrogel); B) Yield stress of each formulation (strain controlled, 0.01-500%) (mean +/-SD; $n \geq 3$); C) Recovery test, showing the evolution of the storage modulus during a complete cycle, namely at-rest state at 22 °C (1% strain for 10 min), printing step at 22 °C (100% strain for 1 min), post printed rest state at 37 °C (1% strain for 5 min) ($n \geq 3$)(the red zone shows increase of temperature from 22 °C to 37 °C).

Yield stress and recovery tests performed to evaluate the printability of chitosan hydrogels are presented in Figure 2B and C respectively. All hydrogels present a yield stress over 100 Pa, CH-Gel exhibiting the lowest and CH3 the highest value (Figure 2B). The yield stress can be considered as a critical stress above which the hydrogel starts to flow, showing the injectability of the material (initial force required to generate flow) [16]. Bioinks that exhibit a large yield stress will also naturally resist deformation and maintain the printed structure, a major advantage for 3D bioprinting [16].

Figure 2C shows the evolution of the storage modulus during recovery tests for each formulation. To mimic the specific recovery conditions of the warm FRESH method, the temperature was increased to 37 °C at the time of shear removal. All hydrogels showed shear thinning under applied stress. For CH2, immediate recovery is observed, with G' reaching similar and rapidly even higher values after shear removal, probably due the fact that gelation occurs at 37°C. In contrast, CH-Gel recovered only after some time, which could be explained by the melting of the gelatin in the

hydrogel. CH3 shows an intermediate behaviour, a few seconds being necessary to reach back the original storage modulus after shear removal.

3.3. Optimization of printing parameters

The hydrogels were printed using a 3D Discovery printer with a 25G needle. Preliminary printing assays were performed on glass substrate to evaluate the influence of the flow rate (varied from 0.5 to 1.5 mm³/s) and feed rate (speed of the printing nozzle (3-11 mm/s)) on the resolution, in terms of the thickness and continuity of the filaments (Figures 3A-C). The best condition (flow rate of 0.5 mm³/min and feed rate of 9 mm/s) was then chosen to print within the Pluronic 19%+1% NaCl FRESH bath) (Figures 3D-F).

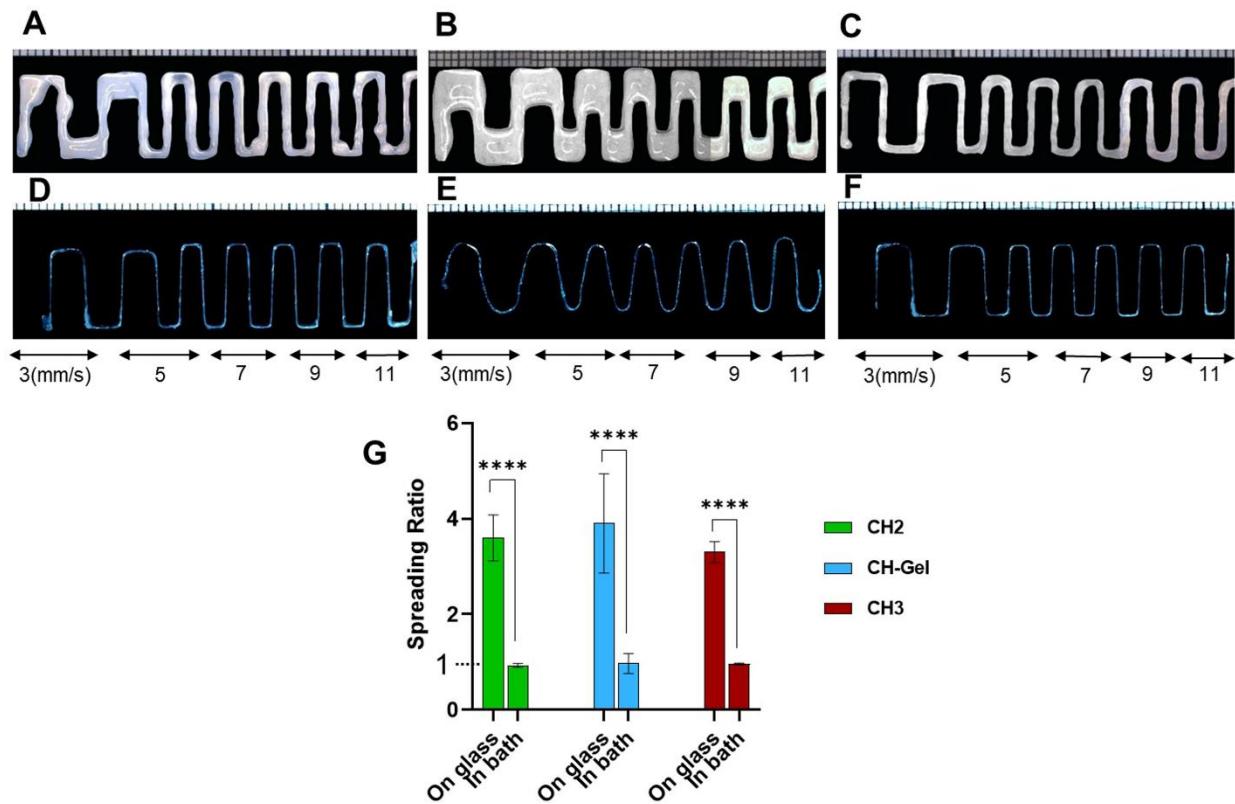


Figure 3. Illustration of how the FRESH method greatly reduces the diameter of printed filaments. Images of filaments printed with a 25G needle (0.26 mm inner diameter) with feed rates changing from 3 to 11 mm/s: A-C: on glass with flow rate of 0.5, 1, 1.5 mm³/s and D-F: within the support bath with flow rate of 0.5 mm³/s for three formulations: 2% chitosan (CH), B) 2%chitosan-2% (w/v) gelatin (CH-Gel), and C) 3% chitosan-based hydrogel (mean \pm -SD; n \geq 3); G) Spreading ratio of the printed filaments with optimized flow rate and feed rate (mean \pm SD; n \geq 3; **** p<0.0001).

As can be seen on Figure 3, printing within the support bath drastically enhances the resolution. The diameter of the printed filament decreased 6, 4, and 5-fold for CH2, CH-GEL, CH3 hydrogels, respectively. The spreading ratio (filament width on needle diameter) was significantly decreased

when hydrogels were printed within the bath (Figure 3G) (**** $p < 0.0001$), the width of the filaments deposited directly within the FRESH bath between 0.2 and 0.3 mm, quite similar to the diameter of the injection needle (25G = 0.26 mm inner diameter). This is in accordance with previous studies using the FRESH approach [38].

3.4. Printed structures on glass and within the FRESH bath

We then evaluated the feasibility of printing a complex multi-layer structure. The gridded structure shown in Figure 4G was printed at 10 layers, both on warm glass and within the warm FRESH bath. Figure 4 presents the resolution and handability of the printed structures after 24 h incubation at 37 °C.

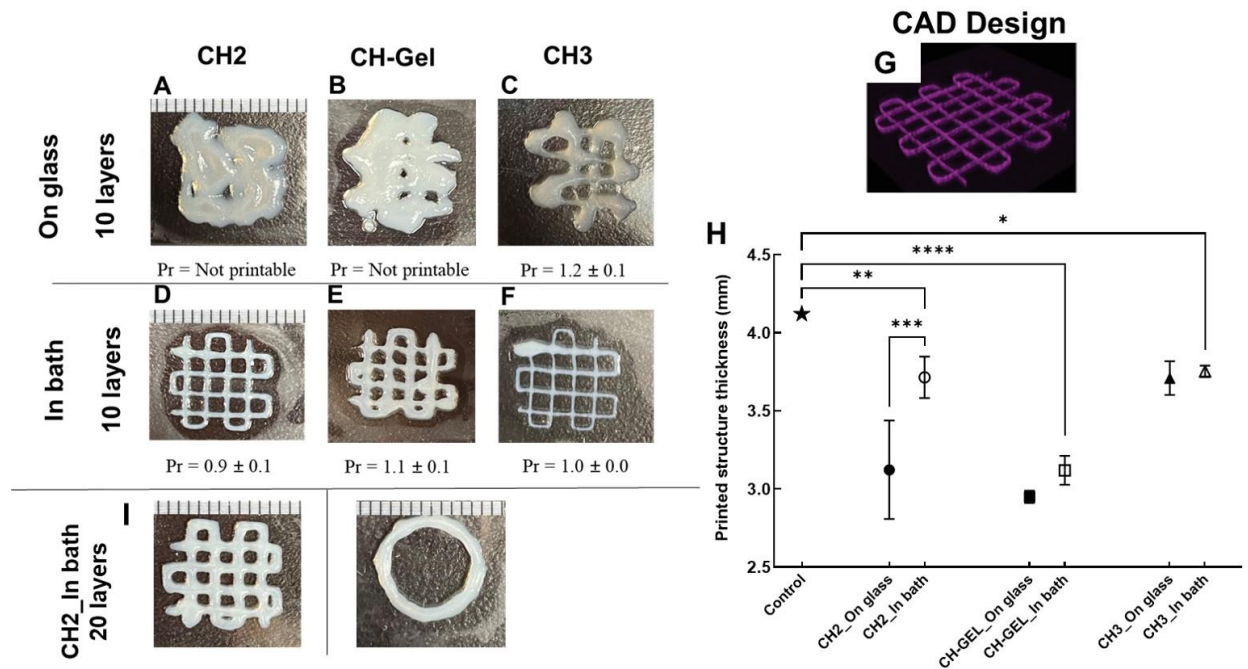


Figure 4. The FRESH method strongly enhances the resolution and feasibility of creating 3D structures with chitosan hydrogels. Pictures of gridded structures after 24 h gelation at 37 °C; A-C) printed on warm glass substrate (10-layers); D-F) printed in the Pluronic support bath (10-layers) ; G) CAD design of the gridded structure (scale 1 cm); H) Thickness of 20-layers printed structures after 24 h gelation at 37 °C, in comparison to the theoretical height (control ★) (mean ± SD; $n \geq 3$); (2% w/v chitosan (CH2), 2% chitosan-2% gelatin (CH-GEL), and C) 3% w/v chitosan (CH3)-based hydrogel (* $p < 0.5$, ** $p < 0.01$, *** $p < 0.001$, **** $p < 0.0001$); I) Pictures of gridded, and cylindrical structures printed in the Pluronic support bath (20-layers) of CH2.

Printing a gridded structure of more than 5 layers was not possible when hydrogels were printed on glass. The layers tended to collapse, especially with CH2 and CH-Gel hydrogels. These limitations are in accordance with previous work published by our team and others [6, 7]. Moreover, structures were very difficult to retrieve from the support. Using the FRESH bath, hydrogels were printable at least up to 20 layers, easy to remove from the substrate, and presented good cohesion, handability and relatively good correspondence to the theoretical CAD design (Figures 4D-F). CH3 showed the best printability, followed by CH2. The resolution of the CH-Gel

hydrogel structure was lower, probably due to diffusion of the gelatin when increasing the temperature to 37 °C, which lead to a temporary decrease of the rheological properties as shown in Figure 2A.

In addition, the thickness of the structures was found to be higher when printed in the bath (Figure 4H). The difference was significant only for CH2 (3.7 ± 0.1 vs 3.1 ± 0.3 mm; $p < 0.001$), whose values were similar to those of CH3 thanks to the support bath. These results suggest that the support bath helped to prevent the filament from spreading out during printing, as well as from collapsing under the weight of the multiple layers. In contrast, CH-Gel structures remain far from the ideal (thickness of 3.1 ± 0.1 vs 4.2 mm for the theoretical value; $p < 0.0001$). Hydrogels printed in support bath showed improved printability in range of $0.9 < Pr < 1.1$ as reported by other teams [30].

3.5. Post-printed mechanical properties

A good bioink should provide tissue-mimicking rigidity and good mechanical strength after printing. The mechanical properties of 20-layer gridded structures, printed either on glass or within the warm FRESH bath, were therefore tested in compression, after 24 h gelation at 37 °C. Figure 5A presents typical curves up to 80% deformation. Since hydrogels present a non-linear behavior, the rigidity is expressed by the secant modulus at 30% deformation on Figure 5B.

The hydrogels printed within the bath were found to have greater rigidity than those printed on the glass. The difference was significant for all hydrogels (Figure 5 B). The difference was particularly notable for CH2, which passed from 1.0 ± 0.2 kPa when printed on glass to 16.3 ± 3.1 kPa when printed in the support bath at 30% deformation. The reason for these enhanced mechanical properties is unclear, but it may be due to a better cohesion between the layers and prevention of evaporation during printing.

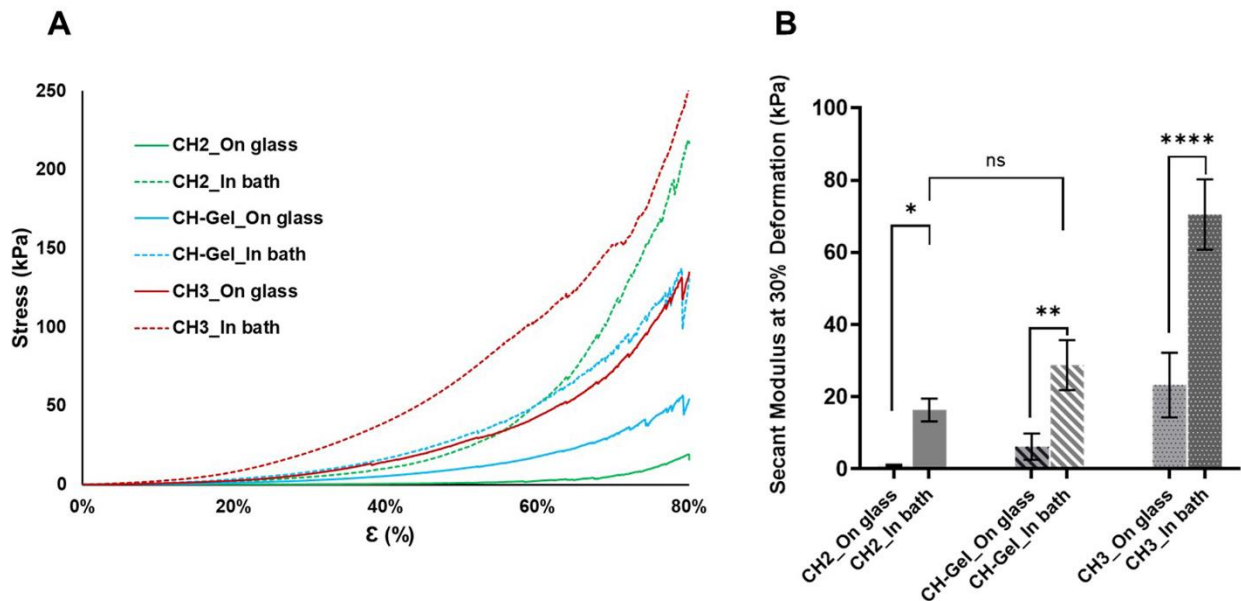


Figure 5. Mechanical properties of 20-layer structures printed on glass and within the FRESH bath: A) stress-strain curve in unconfined compression; B) secant Young's Modulus at 30% deformation (CH2: 2% w/v chitosan, CH3: 3% w/v chitosan; CH-Gel: 2% w/v chitosan-2% w/v gelatin) (mean \pm SD; $n \geq 3$; * $p < 0.05$, ** $p < 0.01$, **** $p < 0.0001$).

More importantly, these results confirm the strong mechanical properties of these chitosan hydrogels. Their secant modulus at 30% deformation reached 16 ± 3 kPa, 28 ± 7 kPa and 70 ± 10 kPa for CH2, CH-Gel and CH3 respectively (Figure 5B), and all sustained deformations up to 80% without breakage (Figure 5A). Such high values can be explained by the presence of SHC in the gelling agent solution. Indeed, it was previously shown that CH gel made with SHC+BGP were drastically stronger than the conventional CH-BGP hydrogels [2, 39, 40]. Replacing part of the BGP with SHC is thought to lead to stronger interactions between the chitosan chains due to the SHC's decomposition into CO_2 during gelation [2] (Equation 3). SHC+BGP hydrogels also make it possible to attain rapid gelation at reduced BGP concentrations, to the benefit of cell survival (more physiological osmolality).



3.6. Cell viability

Preliminary assessment of the compatibility for cell encapsulation showed that CH3 resulted in high cell mortality when cells were encapsulated in this hydrogel (Figure 6), probably because of its high density, as observed by SEM (see Figure S5). For this reason, bioprinting was performed only with CH2 and CH-Gel hydrogels. Figure 7 presents typical live/dead images and cell viability of MSC in bioprinted hydrogels after 24 h, in comparison with hydrogels not submitted to extrusion (control 1) and submitted to the complete process except the FRESH bath and its removal (control 2).

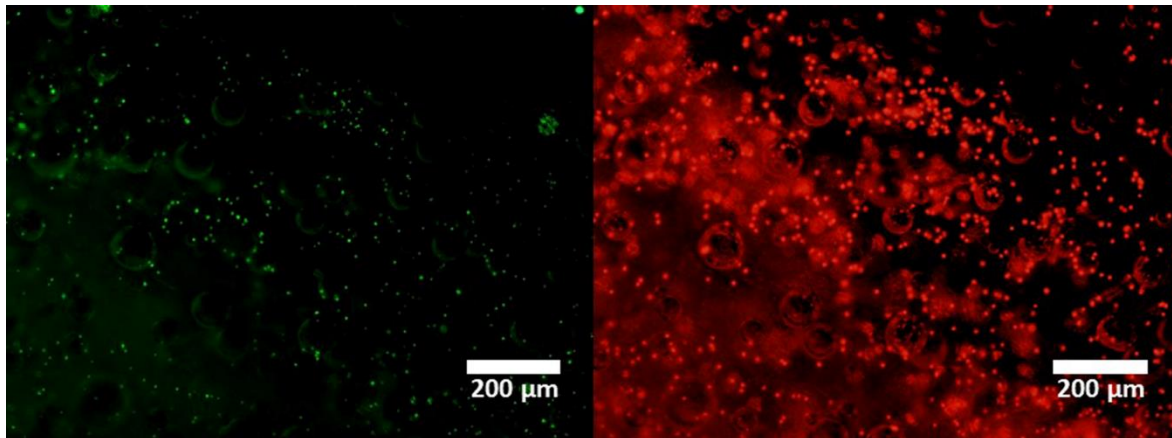


Figure 6. Live-dead assay of L292 fibroblast cells encapsulated in 3% (w/v) chitosan-based hydrogel after 24 h (live cells were stained with Calcein and dead cells were stained with EthD-1).

Results show homogeneous cell distribution in the hydrogels, with good cell viability in CH bioprinted structures (76%), but significantly lower in CH-Gel (52%; $p < 0.001$). In both cases the viability was lower than in the non-printed control (85% and 76% for CH and CH-Gel, respectively), possibly due to the shear stress applied during bioprinting. According to the literature, dead cells and cell damage increase as the pressure and needle length increase [41-43]. Another reason for decreased cell viability is probably the time the cells spend at temperatures $< 37^\circ\text{C}$ and the manipulation prior to the bioprinting process e.g., centrifugation.

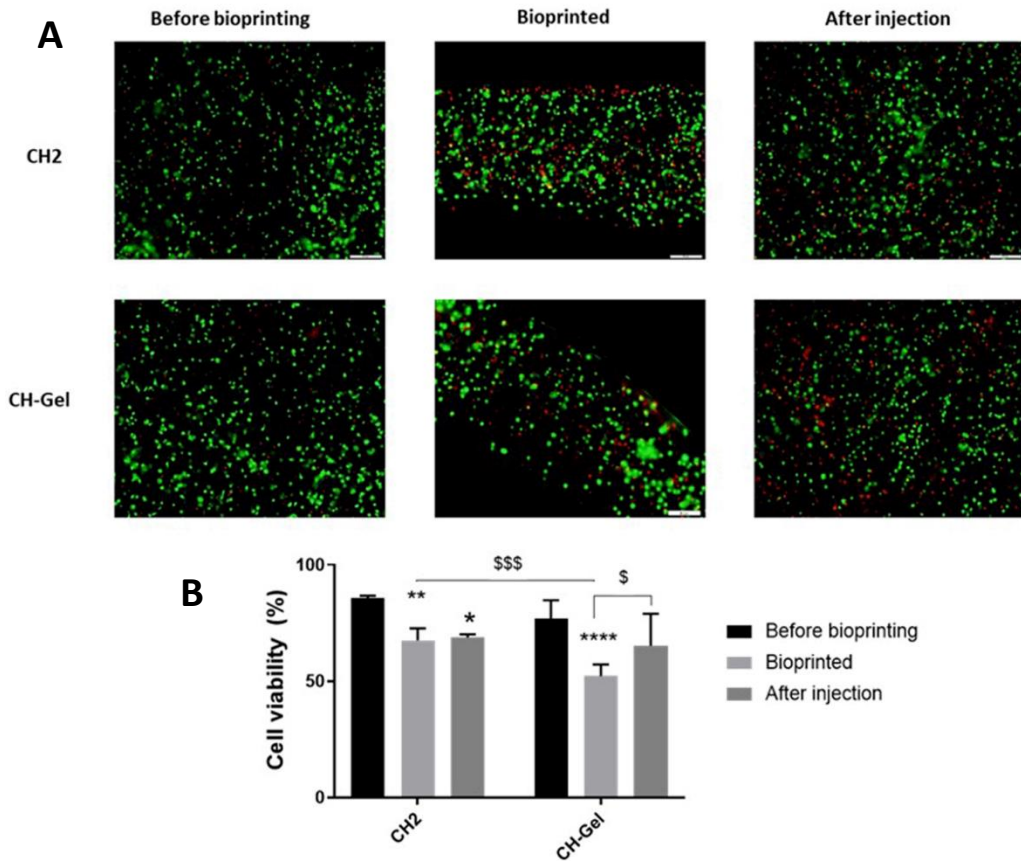


Figure 7. Viability of encapsulated MSCs loaded in CH2 and CH-Gel hydrogels, printed within the support bath A) Live-dead images (Live cells appear in green, dead cells in red); B) percentage of live cells (mean \pm SD; $n > 4$). Controls correspond to hydrogel solutions simply injected in a well before and after the bioprinting process (* $p < 0.05$, ** $p < 0.01$, **** $p < 0.0001$ compared to the control before bioprinting; (\$ $p < 0.05$; \$\$\$ $p < 0.001$, compared to CH-Gel sample) (CH2: chitosan 2% w/v; CH-Gel: chitosan 2% w/v – gelatin 2% w/v) (Live/dead assays).

The cell viability in bioprinted CH2 was similar to that of the second control, which differed only by the presence of the FRESH bath and the bath removal procedure. This suggests that the Pluronic support bath, as well as the few minutes at low temperature required to retrieve it, were not harmful to the encapsulated cells with this formulation. There was a slight difference, however, in the case of CH-Gel.

The slightly lower cell viability in CH-Gel compared to CH2 was not expected since gelatin is known to favor cell adhesion and cell survival in chitosan-based hydrogels [44, 45]. The lower cell viability might be due to the rheological behavior of the bioinks, gelatin escaping during the warm incubation, or the Pluronic bath sticking to the CH-Gel.

Further work is of course needed to study the influence of the bioprinting parameters (shear stress, needle size, needle type etc.), the duration of bioprinting and Pluronic exposure as well as the process of bath removal, on the survival of encapsulated cells.

4. Conclusion

In this work, we demonstrate how using the FRESH approach with a warm support bath at 37 °C drastically enhances the potential of chitosan-based thermosensitive hydrogel as bioinks for 3D bioprinting. Physical CH hydrogels gel in situ at body temperature, but gelation is not immediate, which leads to spreading of printed material and poor resolution when simply printed on a warm substrate. The FRESH method provides mechanical support and assists in adequate thermocrosslinking during printing, while preventing evaporation and easing sample removal.

Chitosan 2%w/v, chitosan 3% w/v and chitosan-gelatin (2-2%) hydrogel bioinks were tested for their rheological properties and printability. Printing in the support bath led to marked improvement of the resolution of the printed 3D structures, in particular for CH2 hydrogel. Structures had good cohesion and handability. They presented strong mechanical properties thanks to the use of a mix of sodium bicarbonate and beta-glycerophosphate as gelling agents.

Despite excellent printing resolution, CH3 was discarded due to its low porosity and low cell survival. CH2 presented better rheological properties, printing behavior and MSC survival than CH-gelatin hydrogel, probably because gelatin escapes from the gel into the support bath at 37 °C. While further study is required to optimize the process, these results show that the main limitation of thermosensitive chitosan-based hydrogels as bioink can be overcome by using the FRESH method. In particular, chitosan 2%w/v formulation appears as a good candidate for 3D FRESH bioprinting for various tissue engineering applications.

Acknowledgements

We would like to thank the Natural Science and Engineering Research Council of Canada (NSERC; RGPIN-2015-05169) and the *Fonds de Recherche du Quebec—Nature et technologie* (FRQNT; team project and M R scholarship) for providing funding for this project. We would like to thank Thierry Labonté-Dupuis for his help with the bioprinter and S.K. Rezvaninejad for his help in producing the figures. The graphical abstract was made using www.biorender.com.

References

1. Chenite, A., et al., *Rheological characterisation of thermogelling chitosan/glycerol-phosphate solutions*. 2001. **46**(1): p. 39-47.
2. Assaad, E., M. Maire, and S. Lerouge, *Injectable thermosensitive chitosan hydrogels with controlled gelation kinetics and enhanced mechanical resistance*. Carbohydrate polymers, 2015. **130**: p. 87-96.
3. Ceccaldi, C., et al., *Optimization of injectable thermosensitive scaffolds with enhanced mechanical properties for cell therapy*. Macromolecular bioscience, 2017. **17**(6): p. 1600435.
4. Monette, A., et al., *Chitosan thermogels for local expansion and delivery of tumor-specific T lymphocytes towards enhanced cancer immunotherapies*. Biomaterials, 2016. **75**: p. 237-249.
5. Alinejad, Y., et al., *An injectable chitosan/chondroitin sulfate hydrogel with tunable mechanical properties for cell therapy/tissue engineering*. 2018. **113**: p. 132-141.
6. Rahimnejad, M., et al., *A rheological approach to assess the printability of thermosensitive chitosan-based biomaterial inks*. Biomedical Materials, 2020. **16**(1): p. 015003.
7. Ku, J., et al., *Cell-laden thermosensitive chitosan hydrogel bioinks for 3D bioprinting applications*. 2020. **10**(7): p. 2455.
8. Maturavongsadit, P., et al., *Cell-Laden Nanocellulose/Chitosan-Based Bioinks for 3D Bioprinting and Enhanced Osteogenic Cell Differentiation*. 2021. **4**(3): p. 2342-2353.
9. Hinton, T.J., et al., *Three-dimensional printing of complex biological structures by freeform reversible embedding of suspended hydrogels*. Science advances, 2015. **1**(9): p. e1500758.
10. Mirdamadi, E., et al., *FRESH 3D Bioprinting a Full-Size Model of the Human Heart*. ACS Biomaterials Science Engineering, 2020. **6**(11): p. 6453-6459.
11. Lee, A., et al., *3D bioprinting of collagen to rebuild components of the human heart*. Science, 2019. **365**(6452): p. 482-487.
12. Haring, A.P., et al., *Process-and bio-inspired hydrogels for 3D bioprinting of soft free-standing neural and glial tissues*. Biofabrication, 2019. **11**(2): p. 025009.
13. McCormack, A., et al., *3D printing in suspension baths: keeping the promises of bioprinting afloat*. Trends in biotechnology, 2020. **38**(6): p. 584-593.
14. Afghah, F., et al., *Preparation and characterization of nanoclay-hydrogel composite support-bath for bioprinting of complex structures*. Scientific reports, 2020. **10**(1): p. 1-13.
15. Mitsoulis, E., S. Abdali, and N. Markatos, *Flow simulation of herschel-bulkley fluids through extrusion dies*. The Canadian Journal of Chemical Engineering, 1993. **71**(1): p. 147-160.
16. Townsend, J.M., et al., *Flow behavior prior to crosslinking: The need for precursor rheology for placement of hydrogels in medical applications and for 3D bioprinting*. Progress in polymer science, 2019. **91**: p. 126-140.
17. Compaan, A.M., K. Song, and Y. Huang, *Gellan fluid gel as a versatile support bath material for fluid extrusion bioprinting*. ACS applied materials & interfaces, 2019. **11**(6): p. 5714-5726.
18. Basu, A., et al., *Catalytically initiated gel-in-gel printing of composite hydrogels*. ACS applied materials & interfaces, 2017. **9**(46): p. 40898-40904.
19. Ning, L., et al., *Embedded 3D Bioprinting of Gelatin Methacryloyl-Based Constructs with Highly Tunable Structural Fidelity*. ACS Applied Materials & Interfaces, 2020. **12**(40): p. 44563-44577.
20. Hinton, T.J., et al., *3D printing PDMS elastomer in a hydrophilic support bath via freeform reversible embedding*. ACS biomaterials science & engineering, 2016. **2**(10): p. 1781-1786.
21. Jin, Y., et al., *Functional nanoclay suspension for printing-then-solidification of liquid materials*. ACS applied materials & interfaces, 2017. **9**(23): p. 20057-20066.
22. Ding, H. and R.C. Chang, *Printability study of bioprinted tubular structures using liquid hydrogel precursors in a support bath*. Applied Sciences, 2018. **8**(3): p. 403.

23. Jatav, S. and Y.M. Joshi, *Phase behavior of aqueous suspension of laponite: New insights with microscopic evidence*. Langmuir, 2017. **33**(9): p. 2370-2377.
24. Rocca, M., et al., *Embedded multimaterial extrusion bioprinting*. SLAS TECHNOLOGY: Translating Life Sciences Innovation, 2018. **23**(2): p. 154-163.
25. Hull, S.M., et al., *3D Bioprinting using UNiversal Orthogonal Network (UNION) Bioinks*. Advanced Functional Materials, 2020: p. 2007983.
26. Ferdows, A., et al., *Preparation and characterization of nanoclay-hydrogel composite support-bath for bioprinting of complex structures*. Scientific Reports, 2020. **10**(1).
27. Bayaniahangar, R., et al., *3-D printed soft magnetic helical coil actuators of iron oxide embedded polydimethylsiloxane*. Sensors and Actuators B: Chemical, 2021. **326**: p. 128781.
28. Jiang, J., et al., *The effect of physiologically relevant additives on the rheological properties of concentrated Pluronic copolymer gels*. Polymer, 2008. **49**(16): p. 3561-3567.
29. Gillispie, G., et al., *Assessment methodologies for extrusion-based bioink printability*. Biofabrication, 2020. **12**(2): p. 022003.
30. Ouyang, L., et al., *Effect of bioink properties on printability and cell viability for 3D bioplotting of embryonic stem cells*. Biofabrication, 2016. **8**(3): p. 035020.
31. Tan, J.J.Y., C.P. Lee, and M. Hashimoto, *Preheating of gelatin improves its printability with transglutaminase in direct ink writing 3D printing*. International Journal of Bioprinting, 2020. **6**(4).
32. Cidade, M., et al., *Injectable hydrogels based on pluronic/water systems filled with alginate microparticles for biomedical applications*. Materials, 2019. **12**(7): p. 1083.
33. Geng, H., et al., *Sustained release of VEGF from PLGA nanoparticles embedded thermo-sensitive hydrogel in full-thickness porcine bladder acellular matrix*. Nanoscale research letters, 2011. **6**(1): p. 1-8.
34. Shriky, B., et al., *Pluronic F127 thermosensitive injectable smart hydrogels for controlled drug delivery system development*. Journal of colloid interface science, 2020. **565**: p. 119-130.
35. Hopkins, C.C. and J.R. de Bruyn, *Gelation and long-time relaxation of aqueous solutions of Pluronic F127*. Journal of Rheology, 2019. **63**(1): p. 191-201.
36. Jiang, J., et al., *The effect of physiologically relevant additives on the rheological properties of concentrated Pluronic copolymer gels*. Polymer, 2008. **49**(16): p. 3561-3567.
37. Roehm, K.D. and S.V. Madihally, *Bioprinted chitosan-gelatin thermosensitive hydrogels using an inexpensive 3D printer*. Biofabrication, 2017. **10**(1): p. 015002.
38. Corbett, D.C., E. Olszewski, and K. Stevens, *A FRESH take on resolution in 3D bioprinting*. Trends in biotechnology, 2019. **37**(11): p. 1153-1155.
39. Lavertu, M., D. Filion, and M.D. Buschmann, *Heat-induced transfer of protons from chitosan to glycerol phosphate produces chitosan precipitation and gelation*. Biomacromolecules, 2008. **9**(2): p. 640-650.
40. Cho, J., et al., *Physical gelation of chitosan in the presence of β -glycerophosphate: the effect of temperature*. Biomacromolecules, 2005. **6**(6): p. 3267-3275.
41. Han, S., et al., *Study of the process-induced cell damage in forced extrusion bioprinting*. Biofabrication, 2021. **13**(3): p. 035048.
42. Boularaoui, S., et al., *An overview of extrusion-based bioprinting with a focus on induced shear stress and its effect on cell viability*. Bioprinting, 2020: p. e00093.
43. Blaeser, A., et al., *Controlling shear stress in 3D bioprinting is a key factor to balance printing resolution and stem cell integrity*. Advanced healthcare materials, 2016. **5**(3): p. 326-333.
44. Mousavi, S., et al., *Comparative study of collagen and gelatin in chitosan-based hydrogels for effective wound dressing: Physical properties and fibroblastic cell behavior*. Biochemical biophysical research communications, 2019. **518**(4): p. 625-631.

45. Re, F., et al., *3D gelatin-chitosan hybrid hydrogels combined with human platelet lysate highly support human mesenchymal stem cell proliferation and osteogenic differentiation*. *Journal of tissue engineering*, 2019. **10**: p. 2041731419845852.

Supporting Information

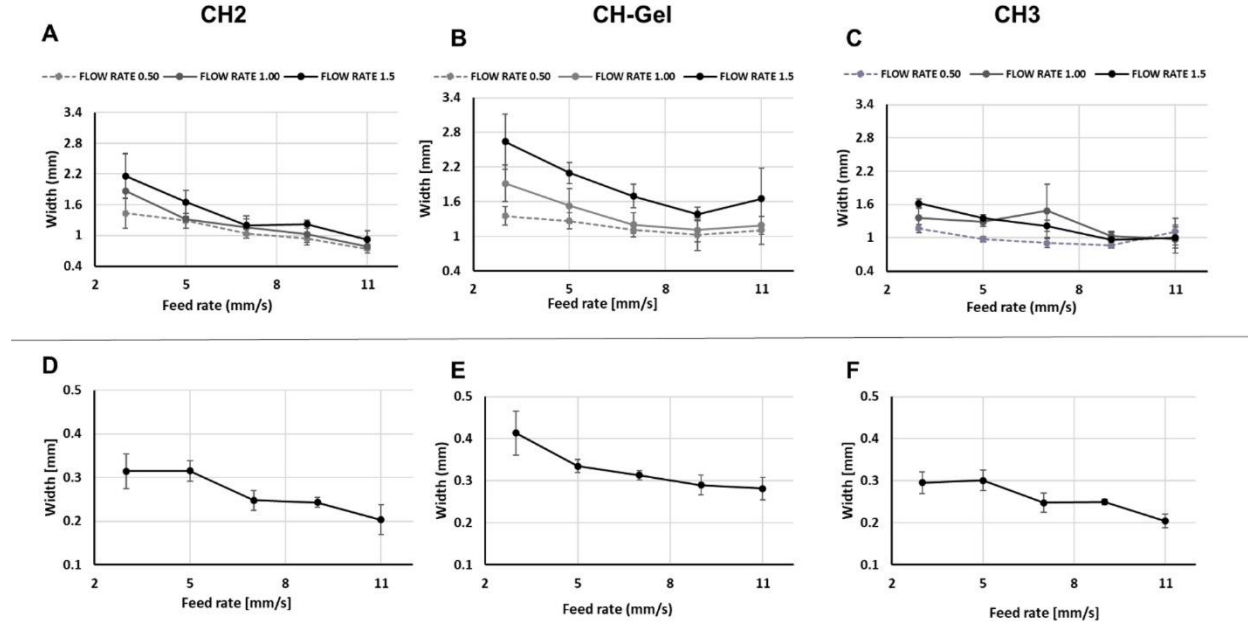


Figure S1. Mean diameter and images of filaments printed with a 25G needle (0.26 mm inner diameter) with feed rates changing from 3 to 11 mm/s: A-C: on glass with flow rate of 0.5, 1, 1.5 mm³/s and D-F: within the support bath with flow rate of 0.5 mm³/s for three formulations: 2% chitosan (CH), B) 2%chitosan-2% (w/v) gelatin (CH-Gel), and C) 3% chitosan-based hydrogel (mean +/-SD; n≥3).

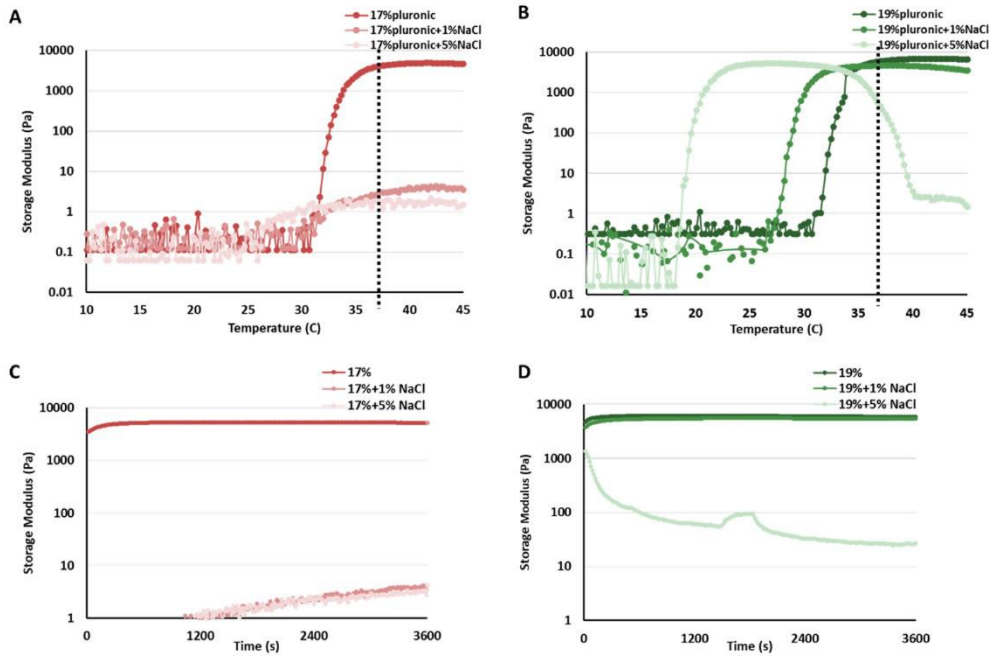


Figure S2. Rheological properties of Pluronic support bath A-B) Effects of added NaCl on temperature ramps (10-45 °C) of Pluronic 17% and 19% (w/v) (dotted line=37°C); C-D) Time sweep of Pluronic bath at 37 °C; (mean; n≥3).

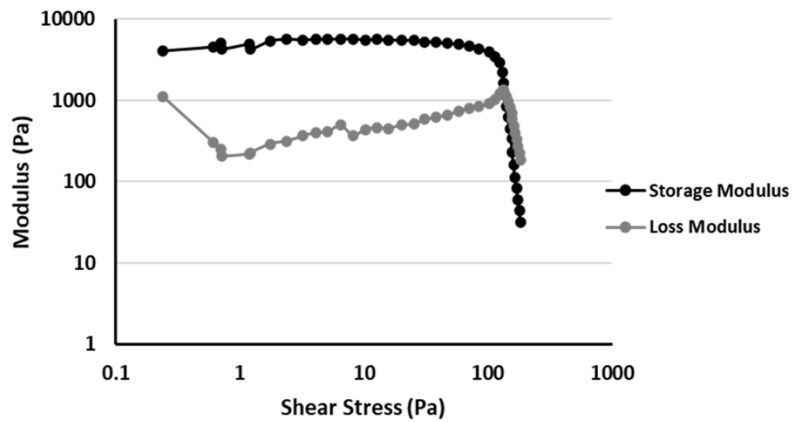


Figure S3. Amplitude sweep, with controlled-shear deformation (0.01%-100%) of Pluronic19% + 1% NaCl at 37 °C; (mean; $n \geq 3$).

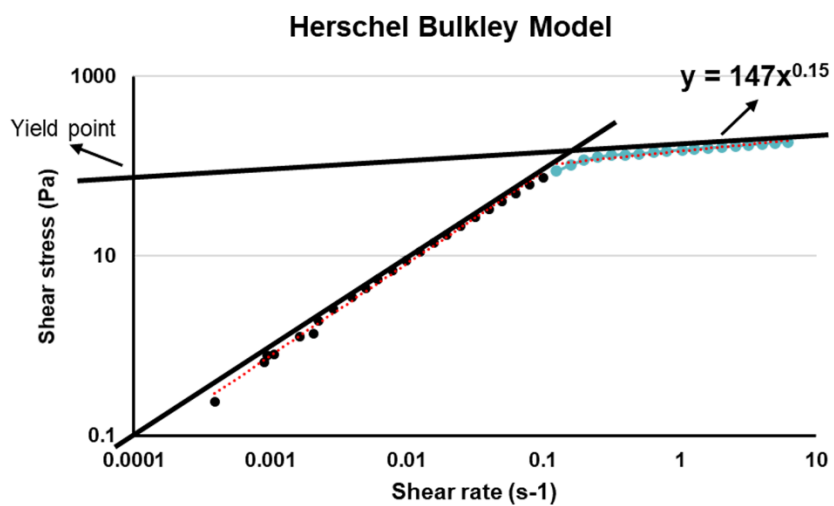


Figure S4. Herschel Bulkley model of the Pluronic + 1% NaCl FRESH support bath (the straight line crossing the Y axis shows the yield stress).

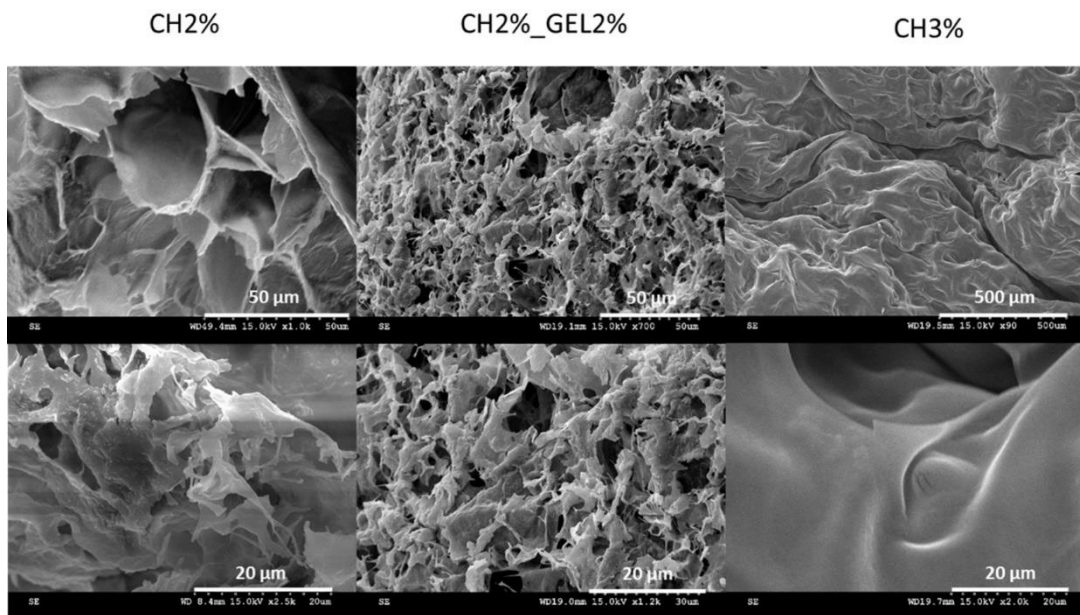


Figure S5. SEM images of CH2%, CH-GEL and CH3% hydrogels.